Ionics (2015) 21:1787–1793
DOI 10.1007/s11581-014-1323-9

ORIGINAL PAPER

A cellulose acetate based nanocomposite for photocatalytic degradation of methylene blue dye under solar light

Vinod Kumar Gupta · Twafik A. Saleh · Deepak Pathania · Bhim Singh Rathore · Gaurav Sharma

Received: 22 October 2014 / Revised: 11 November 2014 / Accepted: 16 November 2014 / Published online: 30 November 2014

Abstract In this work, cellulose acetate–tin (IV) phosphate nanocomposite (CA/TPNC) ion exchanger has been explored for its photocatalytic degradation of methylene blue dye from aqueous solution. The CA/TPNC was characterized using Fourier transform infrared (FTIR) spectroscopy, transmission electron microscopy (TEM) and X-ray diffraction (XRD). The ion exchange capacity of nanocomposite ion exchanger was observed to be high (1.48 meq g^{-1}) for Na^+ ion as compared to their inorganic counterpart (0.56 meq g^{-1}). The CA/TPNC material was the photocatalytic degradation of methylene blue dye onto CA/TPNC was investigated for 140 min of solar irradiation at 662-nm wavelength. The 80 % the dye was removed onto CA/TPNC after 60 min of irradiation. The rate of photodegradation of MB dye onto CA/TPNC followed the pseudo-first-order kinetic model.

V. K. Gupta
Department of Chemistry, Indian Institute of Technology Roorkee, Roorkee 247667, India

V. K. Gupta
Department of Applied Chemistry, University of Johansburg, Johansburg, South Africa

V. K. Gupta (✉) · T. A. Saleh
Chemistry Department, King Fahd University of Petroleum and Minerals, Dhahran, Saudi Arabia
e-mail: vinodfcy@gmail.om

V. K. Gupta
e-mail: vinodfy@iitr.ac.in

D. Pathania · B. S. Rathore · G. Sharma
Department of Chemistry, Shoolini University, Solan, Himachal Pradesh 173212, India

B. S. Rathore
Department of Chemistry, Government P.G. College, Solan, Himachal Pradesh 173212, India

Keywords Cellulose acetate · Nanocomposite · Ion exchange property · Photocatalysis

Introduction

Environmental pollution caused by different toxic pollutants from the domestic use and industrial activity has been of significant concern. Organic pollutants have been added into the water system from industrial effluents, agriculture waste and chemical stumble [1–3]. These pollutants due to toxic, mutagenic and carcinogenic nature cause serious effects to human health. Hence, the removal of the organic dyestuff from waste effluents becomes the focus of important concern. The synthetic dyes have adverse impact on the aquatic submerged plants and resulted in slow photosynthesis process [4–6]. Many organic dyes have complex structures and high resistance to biological oxidation; therefore, it was a great challenge for the decolourization and complete removal from the water system [7, 8]. Many methods such as chemical oxidation, biological treatment, coagulation, flocculation, adsorption, electrochemical, precipitation, adsorption and photocatalysis have been used for the removal of dyes from wastewater [9–23]. However, most of these methods are costly and cannot be effectively used for the treatment of a wide range of organic dye [24]. Photocatalysis has been presently considered as the most efficient method for the removal of the organic dyes from wastewater due to its simplicity, financial practicality, technical feasibility and social suitability [25].

Organic–inorganic nanocomposite ion exchanger has been used in environmental remediation due to their good selectivity and specificity [26, 27]. The remediation of metal ions and dyes from polluted water has been carried out by using several biomaterial-based nanocomposite materials [28–30]. A number of bioadsorbents such as bacterial biomass and biopolymers have been explored for the removal of toxic pollutants from water systems [31, 32]. They are biodegradable, cost

effective, harmless and richly available. Due to low stability, difficulty in separation and low recovery after desorption are the major limitations found in bioadsorbents [33].

Photosensitized degradation of coloured pollutants from wastewater using nanocomposites has been of great significance [34–36]. In recent years, advanced oxidation processes (AOPs) have been suggested as an alternative to conventional methods for the degradation of organic pollutants. AOPs oxidize quickly and non-selectively a broad range of organic pollutants [37, 38]. Heterogeneous photocatalysis via combination of semiconductor and UV light was considered to be one of the promising advanced oxidation processes for the destruction of water-soluble organic pollutants present in wastewater.

In the recent years, our group has been extensively involved for the photocatalytic degradation of dyes using nanocomposite ion exchangers [39, 40]. The outcomes from this research provide great potential of nanocomposite ion exchangers for the treatment of organic pollutant. Until now, no data is available regarding the use of cellulose acetate based tin (IV) phosphate nanocomposite as photocatalyst for the degradation of methylene blue dye from the water system in presence of visible light.

This work deals with the synthesis of cellulose acetate–tin (IV) phosphate nanocomposite (CA/TPNC) ion exchanger by simple sol–gel method. CA/TPNC ion exchanger has been subjected for different spectral analyses. Moreover, the CA/TPNC ion exchanger was investigated for the photocatalytic degradation of methylene blue dye from aqueous medium in presence of sunlight.

Materials and methods

Materials

The reagents tin (IV) chloride and sodium dihydrogen phosphate were procured from Loba Chemia Pvt. Ltd., Mumbai, India. Other chemicals such as formic acid (E. Merck Ltd., India) and cellulose acetate (CDH Pvt. Ltd., New Delhi, India) were used as received. Methylene blue dye was obtained from S. D. Fine Ltd., India. The solutions of desired concentrations were prepared by diluting the stock solution with double-distilled water. The absorbance measurements were recorded on a UV-visible spectrophotometer (Shimadzu UV-1601, Japan).

Synthesis of cellulose acetate–tin (IV) phosphate nanocomposite

Cellulose acetate–tin (IV) phosphate nanocomposite ion exchanger was synthesized using sol-gel method in two steps. In the first step, 0.1 M sodium dihydrogen phosphate solution and 0.1 M tin (IV) chloride solution were mixed with continuous stirring at pH 0–1 as per method discussed earlier [40]. The mixture was stirred for 60 min to obtain tin (IV) phosphate (TP) precipitates. In next step, 4 % (*v*/*v*) cellulose acetate (CA) gel was prepared in concentrated formic acid. The gel was added to tin (IV) phosphate solution with continuous stirring. The resultant mixture was allowed to stand overnight with occasional shaking for digestion. Then, the supernatant liquid was removed and precipitates were washed with demineralized water several times to remove the excess of reagents. The precipitates were converted into H^+ by keeping in 0.1 M HNO_3 solution for 24 h. Then, the precipitates were filtered and washed with demineralized water and finally dried in hot air oven at 50±2 °C.

Ion exchange capacity

The ion exchange capacity of CA/TPNC was determined as per method discussed earlier [40]. In a typical procedure, 1 g of the material in H^+ form was placed in a glass column of 1-cm internal diameter with glass wool support at the bottom. The column was washed with double-distilled water to remove excess of the acid. The H^+ ions from the column of CA/TPNC were eluted with 1.0 M KCl solution. The flow rate was maintained at 0.5 mL min^{-1}. The collected effluent was titrated against a standard alkali solution using phenolphthalein indicator. The hydrogen ions released were calculated using the formula as follows [41, 42]:

$$IEC = \frac{N \times V}{W} \text{mg/g} \quad (1)$$

where *IEC* is ion exchange capacity, *N* and *V* (mL) are the normality and the volume of NaOH, respectively, and *W* (mg) is the weight of CA/TPNC.

Fourier transformer infrared spectra

Fourier transform infrared (FTIR) absorption spectrum of nanocomposite ion exchanger was recorded in the wave number 400–4000 cm^{-1} using a Fourier transform infrared spectrophotometer (Perkin Spectrum-400) using KBr disc method. In this, 10 mg of CA/TPNC in H^+ form was thoroughly mixed with 100 mg of KBr and grounded to very fine powder. The transparent disc was formed by applying the pressure.

Transmission electron microscopy

The particles size and morphology of CA/TPNC ion exchanger were analysed with high-resolution transmission electron microscopy (Hitachi, H7500, Germany).

Photocatalytic activity of cellulose acetate–tin (IV) phosphate nanocomposite

The photocatalytic experiment was carried out in a batch reactor at 30±0.5 °C. In this method, 2×10^{-5} M solution of methylene blue (MB) dye was prepared in double-distilled water, and 100 mg of nanocomposite ion exchanger in H^+ form was added with continuous stirring. In adsorption experiments, slurry composed of dye solution and nanocomposite ion exchanger suspension was stirred magnetically and placed in the dark to establish adsorption–desorption equilibrium. In case of photocatalytic studies, the suspension composed of dye and catalyst was stirred for 15 min and exposed to natural solar light radiations. The 5 mL of solution was withdrawn at different intervals of time and centrifuged. The absorbance was recorded in the range of 300 to 750 nm and kinetics of MB degradation was studied. The percentage degradation of methylene blue dye was calculated using the following formula:

$$\%\text{Degradation} = \frac{C_e - C_t}{Ce} \times 100 \quad (2)$$

where C_e and C_t are the concentration of dye at equilibrium and at time t. The structure on MB is shown below:

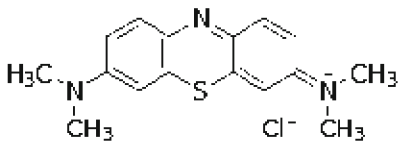

Results and discussion

FTIR analysis

The observed ion exchange capacity for potassium ions was found to be 1.28 meq/g. FTIR spectra of CA/TPNC and CA are shown in Fig. 1a–c. A broad peak observed at 3434 cm^{-1} may be due to presence of external water molecule [43]. Absorption band at 1741 cm^{-1} corresponds to carbonyl group of cellulose acetate in Fig. 1a. The absorption peak at 1633 cm^{-1} was due to free water molecule and strongly bonded –OH group in the matrix. It is observed that peaks 3434, 1741 and 1378 cm^{-1} for CA spectra are shifted to 3432, 1744 and 1376 cm^{-1} spectra of CA/TPNC (Fig. 1b). This shift in the absorption bands confirmed the formation of composite material. The sharp peak at 1039 cm^{-1} may be due to PO_4^{3-}, HPO_4^{2-} and $H_2PO_4^-$ [25]. The absorption peak at 1376 cm^{-1} may be due to vibration of hydroxyl groups. Further, the absorption band at 490 cm^{-1} may be due to superposition of metal-oxygen stretching vibrations confirming the binding between cellulose acetate and tin (IV) phosphate [44]. The marked shift in peak positions from 3432 to 3433 cm^{-1}, 1744 to 1742 cm^{-1}, 1051 to 1053 cm^{-1} and 1633 to 1647 cm^{-1} in the spectra of CA/TPNC and MB dye adsorbed CA/TPNC (Fig. 1c) suggest the interaction of dye molecules with functional groups of nanocomposite.

Transmission electron microscopy analysis

The transmission electron micrographs of CA/TPNC ion exchanger at different magnifications are shown in Fig. 2. The result revealed the wrapping of TP with CA to form the composite material. The TEM images confirmed the formation of particles size in the range of 3–15 nm [45].

Photocatalytic activity of CA/TPNC

The photocatalytic activity of tin (IV) phosphate (TP), cellulose acetate (CA) and cellulose acetate–tin (IV) phosphate nanocomposite (CA/TPNC) were determined for the degradation of methylene blue dye at various parameters as [MB]= 2×10^{-5} M, pH=4.2, catalyst dose=100 mg, time=150 min, wavelength=662 nm. It has been revealed that the decrease in MB absorbance was more in CA/TPNC as compared to TP and CA, which confirmed the more degradation of MB onto composite as shown in Fig. 3.

The high degradation percentage of MB onto CA/TPNC was due to the presence of both the CA and TP in a nanocomposite ion exchanger. Moreover, high photocatalytic activity of CA/TPNC ion exchanger may be due to simultaneous adsorption and photocatalytic activity of composite material [46]. The mechanism of photocatalytic degradation of methylene blue (MB) onto CA/TPNC was shown below.

On irradiation, the conduction band electrons were transferred to the surface of catalyst, producing electron–hole pair (h_{vb}^+/e^-_{CB}). At the conduction band, electrons reduced the O_2 to hydroxyl radicals (OH·). The valance band holes react with OH^-/H_2O and form OH^- radicals [47]. The highly oxidizing OH^- radicals were responsible for the degradation of MB dye. The probable mechanism is as follows:

$$\begin{aligned}
&CA/TPNC + MB \longrightarrow && CA/TPNC\text{-}MB_{ads}\\
&CA/TPNC\text{-}MB_{ads} + hv \longrightarrow && CA/TPNC\text{-}MB^*_{ads}\\
&CA/TPNC\text{-}MB^*_{ads} \longrightarrow && e^-_{CB} + h^+_{VB}\\
&h^+ + H_2O \longrightarrow && \dot{O}H + H^+\\
&O_2 + e^- \longrightarrow && O_2^-\\
&O_2^- + H^+ \longrightarrow && HO_2\\
&2HO_2 \longrightarrow && H_2O_2 + O_2\\
&H_2O_2 + O_2^- \longrightarrow && 2OH + O_2\\
&OH + \text{Methylene blue} \longrightarrow && \text{Degraded product}
\end{aligned}$$

As evident from Fig. 5a, about 60 % of the dye was removed in 20 min of radiation time onto CA/TPNC

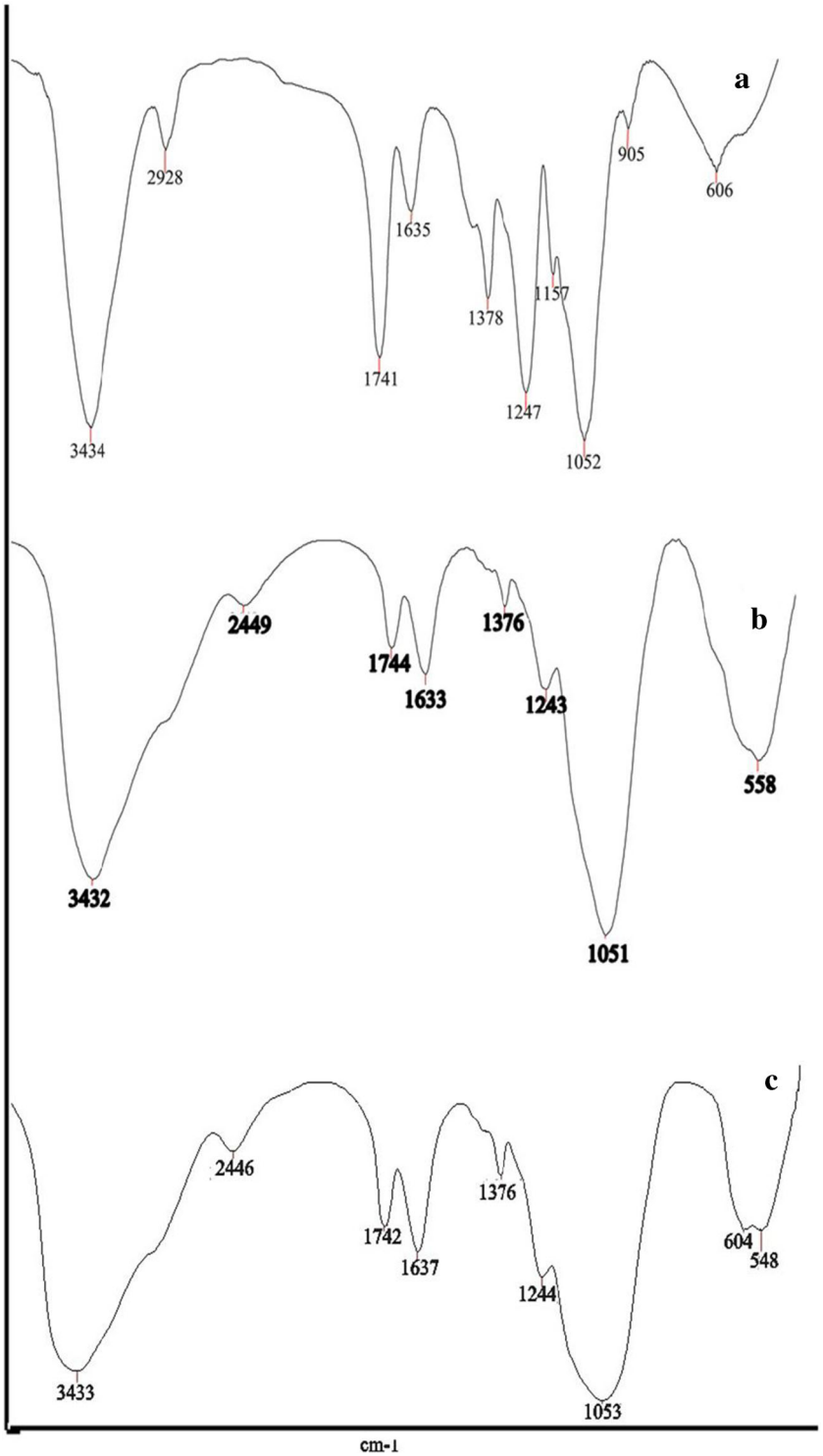

Fig. 1 FTIR spectra. **a** CA, **b** CA/TPNC and **c** CA/TPNC after adsorption of MB

compared to 18 and 5 % degradation of MB onto TP and CA under the same conditions. The photodegradation of dye was elucidated on the basis of decrease in dye concentration both in bulk solution and catalyst surface [48]. The photocatalytic degradation depends on dye concentration in bulk and on the surface of catalyst. It was observed that about 80 % the MB dye was degraded onto CA/TPNC after 60 min of irradiation.

The photodegradation of MB dye was studied under different conditions—equilibrium adsorption in the dark, simultaneous adsorption and degradation, and equilibrium adsorption followed by photodegradation onto TP, CA and CA/TPNC in presence of solar radiation. For the equilibrium adsorption in the dark, only 8, 3 and 45 % degradation was recorded within 20 min of irradiation for TP, CA and CA/

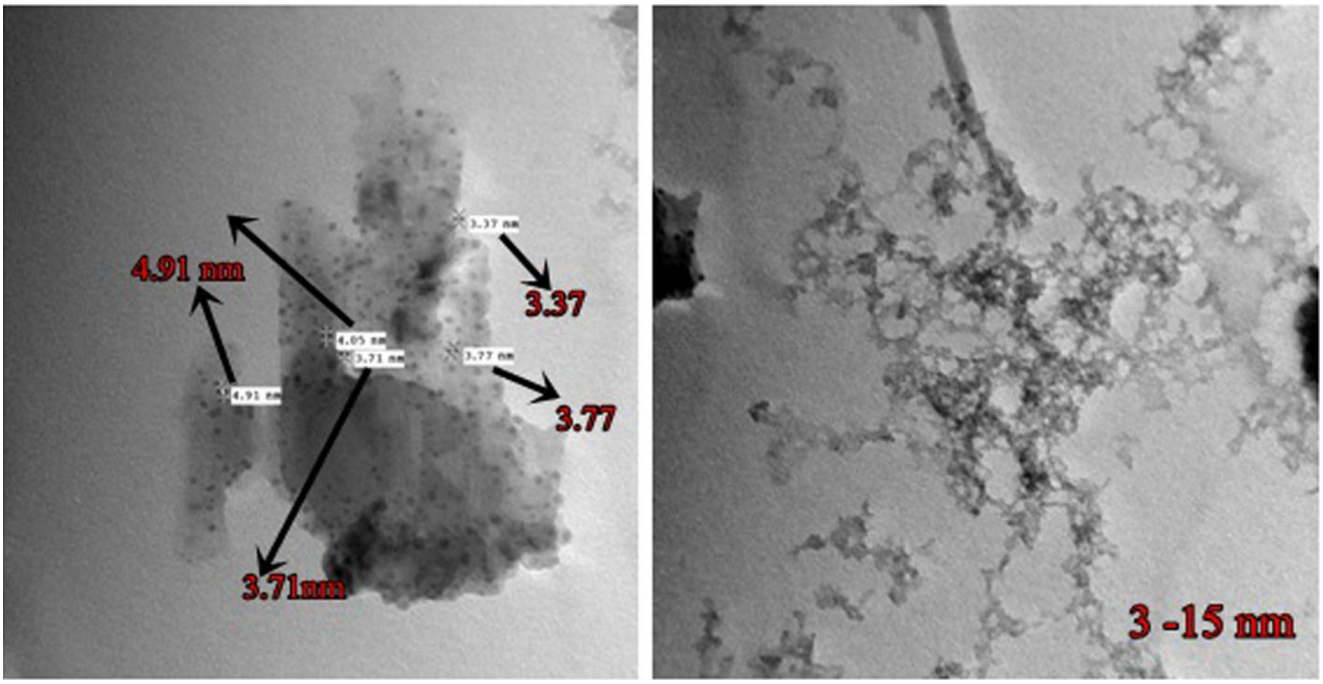

Fig. 2 TEM micrograph of CA/TPNC ion exchanger at different magnifications

TPNC (Fig. 4a). In simultaneous adsorption and degradation (Fig. 3), the MB dye degradation onto different catalysts was 18, 5 and 60 % for TP, CA and CA/TPNC, respectively. In case of simultaneous adsorption followed by photodegradation process (Fig. 5), the instant amount of dye adsorbed onto the surface of catalysts was not very high due to screening effect of sunlight and provided sufficient active sites to generate valance band holes and conduction band electrons [49].

The photocatalytic degradation of dyes obeyed pseudo-first-order kinetic model and the rate of degradation was calculated as follows [50]:

$$r = -\frac{dc}{dt} = k_{app}t \tag{3}$$

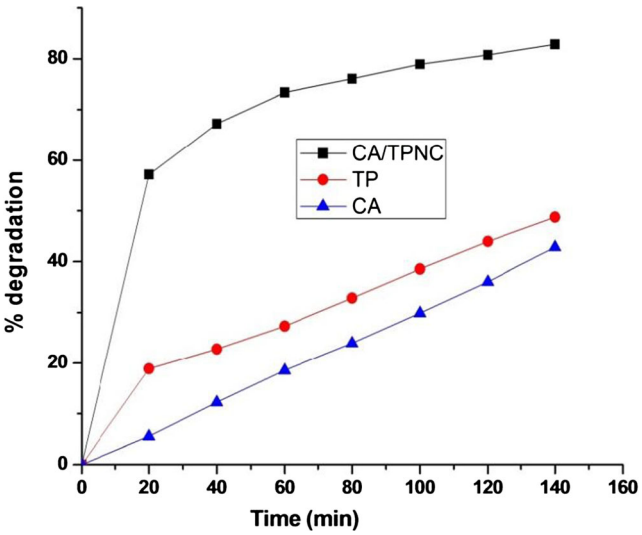

Fig. 3 Photocatalytic degradation of methylene blue dye onto CA, TP and CA/TPNC in presence of solar light at different experimental conditions: initial dye concentration = 2×10^{-5} M, pH=4.2, catalyst dose= 100 mg, time=150 min and wavelength=662 nm

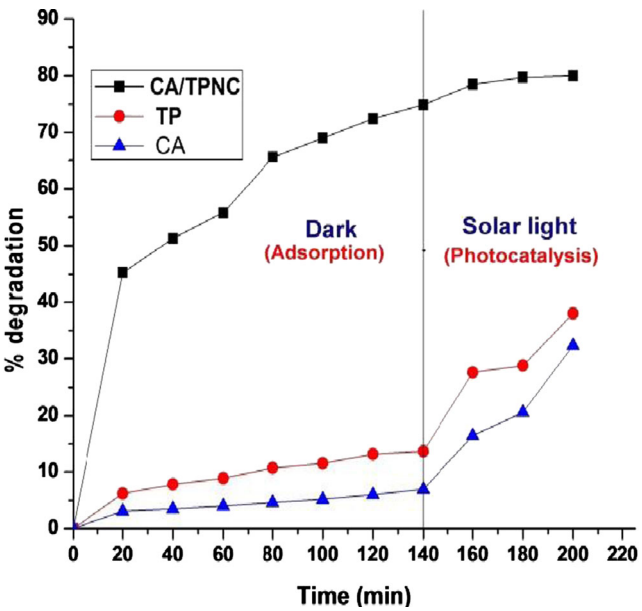

Fig. 4 Equilibrium adsorption followed by photocatalytic degradation onto TP, CA and CA/TPNC in the presence of solar light at different experimental conditions: [MB] = 2×10^{-5} M, pH = 4.2, catalyst dose = 100 mg, time = 150 min and wavelength = 662 nm

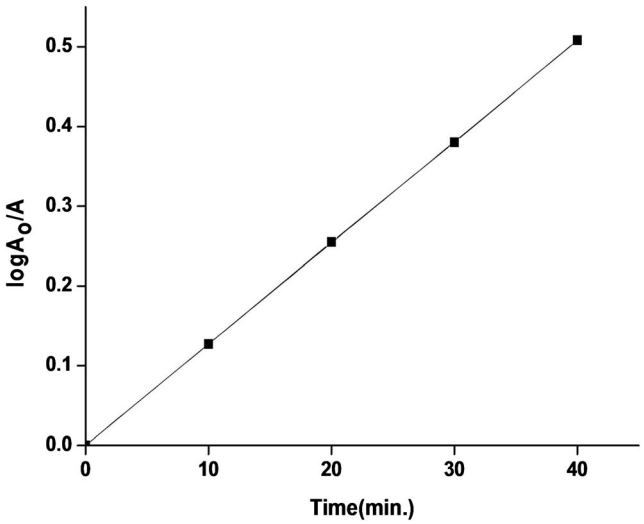

Fig. 5 Kinetics of MB dye degradation onto CA/TPNC ion exchanger

On integrating the above equation, we get

$$\ln C_o/C_t = K_{app}t \quad (4)$$

where K_{app} is the apparent rate constant, C_0 is the concentrations of dye before radiation and C_t is the concentration of dye at time t. The plot of $\ln C_o/C_t$ versus irradiation time resulted in linear correlation with good precision as shown in Fig. 5. Thus, the photodegradation of MB dye using nanocomposite ion exchanger was fitted well in pseudo-first-order kinetics. The value of rate constant $K = 0.0126\ min^{-1}$ was calculated from the slope of the plot with $R^2 = 0.9998$.

Conclusion

In the present study, the synthesized cellulose acetate–tin (IV) phosphate nanocomposite (CA/TPNC) ion exchanger has been successfully explored for the photocatalytic degradation of methylene blue from wastewater. The different spectral analyses confirmed the formation of nanocomposite material. CA/TPNC exhibited high ion exchange capacity with significant photocatalytic activity compared to their counterparts. The simultaneous adsorption and photocatalytic processes proved to be highly efficient for the degradation of methylene blue dye.

References

1. Eren Z, Acar FN (2006) Adsorption of reactive black 5 from an aqueous solution equilibrium and kinetic studies. Desalination 194: 1–10
2. Gupta VK, Mittal A, Mittal J (2010) Decoloration treatment of a hazardous triaryl methane dye, light green SF (yellowish) by waste material adsorbents. J Colloid Interface Sci Z4:2518–527
3. Pathania D, Sharma G, Kothiyal NC, Kumar A (2014) Fabrication of nanocomposite polyaniline zirconium(IV) silicophosphate for photocatalytic and antimicrobial activity. J Alloys Compd 588:668–675
4. Korbahti BK, Artut K, Gecgel C, Ozer A (2011) Electrochemical decolorization of textile dyes and removal of metal ions from textile dye and metal ion binary mixtures. Chem Eng J 173:677
5. Cardoso NF, Pinto RB, Lima EC, Calvete T, Amavisca CV, Royer B, Cunha ML, Fernandes THM, Pinto IS (2011) Removal of remazol black B textile dye from aqueous solution by adsorption. Desalination 269:92–103
6. Gupta VK, Jain R, Mittal A, Agarwal S, Sikarwar S (2012) Photocatalytic degradation of toxic dye amaranth on TiO2/UV in aqueous suspensions. Mater Sci Eng C 32:12–17
7. Kanta S, Pathania D, Singh P, Dhiman P, Kumar A (2014) Removal of malachite green and methylene blue by $Fe_{0.01}/Ni_{0.01}Zn_{0.98}O$/polyacrylamide nanocomposite using coupled adsorption and photocatalysis. Applie Cataly B: Envir 147:340–352
8. Gupta VK, Pathania D, Asif M, Sharma G (2014) Liquid phase synthesis of pectin–cadmium sulfide nanocomposite and its photocatalytic and antibacterial activity. J Mol Liq 196:107–112
9. Sanghavi BJ, Sitaula S, Griep MH, Karna SP, Ali MF, Swami NS (2013) Real-time electrochemical monitoring of adenosine triphosphate in the picomolar to micromolar range using graphene-modified electrodes. Anal Chem 85(17):8158–8165
10. Saleh TA, Gupta VK (2012) Column with CNT/Magnesium oxide composite for lead (II) removal from water. Environ Sci Pollut Res 19:1224–1228
11. Gupta VK, Srivastava SK, Mohan D, Sharma S (1998) Design parameters for fixed bed reactors of activated carbon developed from fertilizer waste material for the removal of some heavy metal ions. Waste Manag 17:517–522
12. Gupta VK, Mittal A, Mittal J (2010) Decoloration treatment of a hazardous triaryl methane dye, light green SF (yellowish) by waste material adsorbents. J Colloid Interface Sci 342:518–527
13. Gupta VK, Mittal A, Kaur D, Malviya A, Mittal J (2009) Adsorption studies on the removal of colouring agent phenol red from wastewater using waste materials as adsorbents. J Colloid Interface Sci 337: 345–354
14. Mittal A, Malviya A, Mittal J, Gupta VK (2009) Adsorptive removal of hazardous anionic dye 'Congo Red' from wastewater using waste materials and recovery by desorption. J Colloid Interface Sci 340:16–26
15. Gupta VK, Agarwal S, Saleh TA (2011) Synthesis and characterization of alumina-coated carbon nanotubes and their application for lead removal. J Hazardous Mat 185:17–23
16. Gupta VK, Ali I, Saleh TA, Nayak A, Agarwal S (2012) Chemical treatment technologies for wastewater recycling—a review. RSC Advances 2:6380–6388
17. Gupta VK, Mittal A, Mittal J (2010) Removal and recovery of chrysoidine Y from aqueous solutions by waste materials. J Colloid Interface Sci 344:497–507
18. Sanghavi BJ, Mobin SM, Mathur P, Lahiri GK, Srivastava AK (2013) Biomimetic sensor for certain catecholamines employing copper(II) complex and silver nanoparticle modified glassy carbon paste electrode. Biosens Bioelectron 39:124–132
19. Sanghavi BJ, Srivastava AK (2010) Simultaneous voltammetric determination of acetaminophen, aspirin and caffeine using an in situ surfactant-modified multiwalled carbon nanotube paste electrode. Electrochim Acta 55:8638–8648
20. Sun H, Liu S, Liu S, Wang S (2014) A comparative study of reduced graphene oxide modified TiO2, ZnO and Ta2O5 in visible light photocatalytic/photochemical oxidation of methylene blue. Appl Catal B 146:162–168

21. Chu W, Tsui SM (1999) Photo-sensitization of diazo disperse dye in aqueous acetone. Chemosphere 39:1667–1677
22. Gupta VK, Pathania D, Kothiyal NC, Sharma G (2014) Polyaniline zirconium (IV) silicophosphate nanocomposite for remediation of methylene blue dye from waste water. J of Mol Liquid 190:139–145
23. Gupta VK, Sharma G, Pathania D, Kothiyal NC (2014) Nanocomposite pectin Zr (IV) selenotungstophosphate for adsorptional/photocatalytic remediation of methylene blue and malachite green dyes from aqueous system. J Ind Eng Chem. doi:10.1016/j.jiec.2014.05.001
24. Pathania D, Kalia S, Sharma R (2012) Graft copolymerization of acrylic acid onto gelatinized patato starch for removal of metal ions and organic dyes from aqueous system. Adv Mat Lett 3:259–264
25. Gupta VK, Pathania D, Sharma S, Singh P (2013) Preparation of bio-based porous carbon by microwave assisted phosphoric acid activation and its use for adsorption of Cr(VI). J Collo Interf Sci 401:125–132
26. Sharma G, Pathania D, Naushad M, Kothiyal NC (2014) Fabrication, characterization and antimicrobial activity of polyaniline Th (IV) tungstomolybdophosphate nanocomposite material: efficient removal of toxic metal ions from water. Chem Eng J 251:413–421
27. Siddiqi ZM, Pathania D (2003) Titanium(IV) tungstosilicate and titanium(IV) tungstophosphate: two new inorganic ion exchangers. J Chromatog A 987:147–158
28. Dong F, Sun Y, FU M, Wu Z, Lee SC (2012) Room temperature synthesis and highly enhanced visible light photocatalytic activity of porous BiOI/BiOCl composites nanoplates microflowers. J Hazard Mater 219:26–34
29. Huang SH, Chen DH (2009) Rapid removal of heavy metal cations and anions from aqueous solutions by an amino-functionalized magnetic nano-adsorbent. J Hazard Mater 163:174–179
30. Gupta VK, Pathania D, Singh P, Kumar A, Rathore BS (2014) Adsorptional removal of methylene blue by guar gum–cerium (IV) tungstate hybrid cationic exchanger. Carbohy Poly 101:684–691
31. Jawad AH, Nawi MA (2012) Oxidation of crosslinked chitosan-epichlorohydrine film and its application with TiO2 for phenol removal. Carbohyd Polym 90:87–94
32. Gupta VK, Pathania D, Agarwal S, Singh P (2012) Adsorptional photocatalytic degradation of methylene blue onto pectin–CuS nanocomposite under solar light. J Hazard Mater 243:179
33. Khan MA, Han DH, Yang OB (2009) Enhanced photoresponse towards visible light in Ru doped titania nanotube. Appl Surf Sci 255:3687–3690
34. Qourzal S, Tamimi M, Assabbane A, Ichou YA (2005) Photocatalytic degradation and adsorption of 2-naphthol on suspended TiO2 surface in a dynamic reactor. J Colliod Interf Sci 286:621–626
35. Jo WK, Shin SH, Wang ESH (2011) Removal of dimethyl sulfide utilizing activated carbon fiber-supported photocatalyst in continuous-flow system. J Hazard Mater 191:234
36. Jianpeng L, Fengqiang S, Kaiyuan G, Tianxing W, Wei Z, Weishan L, Shufang H (2011) Preparation of spindly CuO micro-particles for photodegradation of dye pollutants under a halogen tungsten lamp. Appl Catal A 406:51–58
37. Sano T, Puzenat E, Guillard C, Geantet C, Matsuzawa S (2008) Degradation of C_2H_2 with modified-TiO2 photocatalysts under visible light irradiation. J Mol Catal A Chem 284:127
38. Gupta VK, Agarwal S, Pathania D, Kothiyal NC, Sharma G (2013) Use of pectin–thorium (IV) tungstomolybdate nanocomposite for photocatalytic degradation of methylene blue. Carbohyd Polym 96:277–283
39. Gupta VK, Pathania D, Singh P, Rathore BS (2013) Paryanka chauhan, cellulose acetate-zirconium (IV) phosphate nanocomposite ion exchanger with photocatalytic activity. Carbohyd Polym 95:434–440
40. Rathore BS, Sharma G, Pathania D, Gupta VK (2014) Synthesis, characterization and antibacterial activity of cellulose acetate-tin (IV) phosphate nanocomposite. Carbohydr Polym 103:221–227
41. Sharma G, Pathania D, Naushad M (2014) Preparation, characterization and antimicrobial activity of biopolymer based nanocomposite ion exchanger pectin zirconium (IV) selenotungstophosphate: application for removal of toxic metals. J Ind Eng Chem 20(6):4482–4490
42. Gupta VK, Pathania D, Agarwal S, Sharma S (2012) De-coloration of hazardous dye from water system using chemically modified *Ficus carica* adsorbent. J Mol Liq 174:86
43. Nabi SA, Naushad M (2008) Synthesis, characterization and analytical applications of a new composite cation exchanger cellulose acetate-Zr(IV) molybdophosphate. Synthesis, Colloids Surf A 316:217–225
44. Xu TL, Cai Y, Shea KE (2007) Adsorption and photocatalyzed oxidation of methylated arsenic species in TiO2 suspensions. Environ Sci Tech 41:5471–5477
45. Rathore BS, Sharma G, Pathania D (2013) Photocatalytic activity of cellulose acetate-tin (IV) molybdate nanocomposite in solar light. SMC Bulletin 4:11–16
46. Sillanppa MET, Kurniawasn TA, Lo WL (2011) Degradation of chelating agents in aqueous solution using advanced oxidation process (AOP). Chemosphere 83:1443–1460
47. Hu C, Tang Y, Yu JC, Wong PK (2003) Photocatalytic degradation of cationic blue X-GRL adsorbed on TiO2/SiO2 photocatalyst. Appl Catal, B 40:131–140
48. Gupta VK, Jain R, Varshney S (2007) Removal of reactofix golden yellow 3 RFN from aqueous solution using wheat husk—an agricultural waste. J Hazard Mater 142:443–448
49. Rupa AV, Manikandan D, Divakar D, Sivakumar T (2007) Effect of deposition of Ag on TiO2 nanoparticles on the photodegradation of reactive yellow-17. J Hazard Mater 147:906
50. Xu J, Ao Y, Fu D, Yuan C (2008) Low-temperature preparation of F-doped TiO_2 film and its photocatalytic activity under solar light. Appl Surf Sci 254:3033